

The N³LO Scheme-invariant QCD Evolution of the Non-singlet Structure Functions $F_2^{\text{NS}}(x, Q^2)$ and $g_1^{\text{NS}}(x, Q^2)$

J. Blümlein and M. Saragnese

*Deutsches Elektronen-Synchrotron, DESY,
Platanenallee 6, D-15738 Zeuthen, Germany*

Abstract

We present the scheme-invariant unpolarized and polarized flavor non-singlet evolution equation to N³LO for the structure functions $F_2(x, Q^2)$ and $g_1(x, Q^2)$ including the charm- and bottom quark effects in the asymptotic representation. The corresponding evolution is based on the experimental measurement of the non-singlet structure functions at a starting scale Q_0^2 . In this way the evolution does only depend on the strong coupling constant $\alpha_s(M_Z)$ or the QCD scale Λ_{QCD} and the charm and bottom quark masses m_c and m_b and provides one of the cleanest ways to measure the strong coupling constant in future high luminosity deep-inelastic scattering experiments. The yet unknown parts of the 4-loop anomalous dimensions introduce only a marginal error in this analysis.

1 Introduction

The measurement of the strong coupling constant $\alpha_s(M_Z)$ from precision data on deep-inelastic scattering is one of the cleanest ways to obtain this fundamental parameter of the Standard Model. The present world data allow measurements of $\delta\alpha_s(M_Z)/\alpha_s(M_Z)$ at the level of $\sim O(1\%)$, [1–3]. In the standard analyses one is fitting the scaling violations of deep-inelastic structure functions and obtains $\alpha_s(M_Z)$ together with the parameters of the parton distribution functions, observing the correlation of all parameters, cf. [4]. Compared to this, the measurement of $\alpha_s(M_Z)$ from $R_{e^+e^-}$, cf. [5], does not need to fit a larger amount of further parameters. The different precision determinations of $\alpha_s(M_Z)$ using different processes do not yet agree and further precision measurements are therefore needed.

For deep-inelastic scattering a direct determination of $\alpha_s(M_Z)$ is also possible in the case the starting distributions of the evolution are measured experimentally. In the flavor non-singlet case the corresponding non-singlet structure functions at a scale Q_0^2 provide the input and the data at $Q^2 > Q_0^2$ are fitted to a physical evolution function, which only depends on $\alpha_s(M_Z)$, provided that the input for the values of the heavy quark masses m_c and m_b is known at high precision, as also required in the measurement of $\alpha_s(M_Z)$ from $R_{e^+e^-}$. Here Q^2 denotes the virtuality of the exchanged gauge boson. Therefore scheme-invariant evolution equations allow for a direct determination of the strong coupling constant using measured one dimensional input distributions which are here functions of the Bjorken variable x . An analysis of this kind has been performed in Ref. [6] in the unpolarized case, effectively up to N³LO, however, only considering massless quarks with some further assumptions, see also Ref. [7]. The sensitivity of the structure function on $\alpha_s(M_Z)$ or Λ_{QCD} is traditionally illustrated by the slope $\partial \ln(F_i(x, Q^2))/\partial \ln(Q^2)$ determined experimentally [8–10].

In the present paper we complete the formalism by the single- and double-mass heavy flavor corrections for the Wilson coefficients up to three-loop order and provide numerical results for these effects, using the results given in Refs. [11–17]¹, as well as the massless contributions. Scheme-invariant evolution is usually performed in Mellin N space for technical reasons, because it is simpler in analytic form compared to the corresponding z -space representation. In the polarized case the reference to factorization scheme-invariant quantities will also solve the associated γ_5 problem, which usually arises performing the loop calculation in $D = 4 + \varepsilon$ space-time dimensions. The strong coupling constant is used in the $\overline{\text{MS}}$ scheme. A main goal of the present study is to outline the different evolution effects for high precision measurements.

The measurement of scaling violations concerns that of massless parton evolution and is there implied by the ultraviolet singularity of the respective twist-2 local operators. Referring to the scale evolution using observables necessarily requests to map to the massless partons, which implies in N space the algebraic use of the Wilson coefficients, already at the hard scale Q^2 , as an obstacle, which are different for the various hard processes. For the latter ones it has to be guaranteed that only twist-2 terms contribute, cf. [7, 19, 20], by putting the cuts $W^2 > 15 \text{ GeV}^2, Q^2 > 10 \text{ GeV}^2$, where W is the hadronic mass. The natural scale of evolution in deep-inelastic scattering is Q^2 .

The evolution equation is solved analytically and one final numerical contour integral around the singularities of the corresponding problem delivers the evolved flavor non-singlet structure function in x space. We first consider the flavor decomposition to provide realistic input distributions and derive the corresponding evolution operators for the structure function. Here we also discuss the remainder systematics of the yet not completely known four-loop non-singlet splitting functions $P^{\text{NS},(3),\pm}$. Finally we are providing numerical results in the unpolarized and

¹A numeric implementation of the heavy flavor Wilson coefficients to two-loop order has been given in [18].

polarized case. Precision analyses of this kind can be performed in the physics programme at the future collider experiments at the EIC [21] and LHeC [22].

2 Flavor Decomposition

Since the evolution for the three different flavor non-singlet distributions and the singlet evolution are different, the experimental input at the starting scale Q_0^2 has to be projected correspondingly by combining different deep-inelastic structure functions. One may refer to the following well-known decomposition, see also [23]. Let

$$v_{k^2-1}^\pm = \sum_{l=1}^k (q_l \pm \bar{q}_l) - k(q_k \pm \bar{q}_k), \quad (1)$$

with q_i the quark distributions and

$$v_1^\pm = 0 \quad (2)$$

$$v_3^\pm = (u \pm \bar{u}) - (d \pm \bar{d}) \quad (3)$$

$$v_8^\pm = (u \pm \bar{u}) + (d \pm \bar{d}) - 2(s \pm \bar{s}), \quad (4)$$

one has

$$q_i + \bar{q}_i = \frac{1}{N_F} \Sigma - \frac{1}{i} v_{i^2-1}^+ + \sum_{l=i+1}^{N_F} \frac{1}{l(l-1)} v_{l^2-1}^+, \quad (5)$$

$$\Sigma = \sum_{l=1}^{N_F} (q_l + \bar{q}_l). \quad (6)$$

The nucleon structure functions for pure photon exchange in the case of three light flavors (u, d, s) are then given at leading order (LO) by

$$F_2^p = x \left[\frac{2}{9} \Sigma + \frac{1}{6} v_3^+ + \frac{1}{18} v_8^+ \right] \quad (7)$$

$$F_2^d = \frac{1}{2} [F_2^p + F_2^n] = x \left[\frac{2}{9} \Sigma + \frac{1}{18} v_8^+ \right]. \quad (8)$$

A synonymous decomposition applies to the structure functions xg_1^p and xg_1^d . To project onto the singlet distribution Σ directly one usually needs charged current structure functions, as measured in neutrino experiments [24] or at facilities like the planned LHeC project [22] or the EIC [21] in the unpolarized and polarized case, at high luminosity, with [25]

$$\frac{1}{2} [W_2^{p,+} + W_2^{p,-}] = x \Sigma \quad (9)$$

above the charm threshold [26]. Here the index \pm denotes the exchange of a W^+ or a W^- boson, respectively. Otherwise additional information on sea-quarks is necessary. The flavor non-singlet combinations we are considering are given by

$$F_2^{\text{NS}} = F_2^p - F_2^d = \frac{1}{6} x C_q^{\text{NS},+} \otimes v_3^+ \quad (10)$$

$$xg_1^{\text{NS}} = xg_1^p - xg_1^d = \frac{1}{6}x\Delta C_q^{\text{NS},+} \otimes \Delta v_3^+, \quad (11)$$

where the Wilson coefficients are C_q and ΔC_q contain light and heavy flavor contributions, and \otimes denotes the Mellin convolution

$$[A \otimes B](x) = \int_0^1 dx_1 \int_0^1 dx_2 \delta(x - x_1 x_2) A(x_1) B(x_2). \quad (12)$$

The Mellin transform

$$\mathbf{M}[f(x)](N) = \int_0^1 dx x^{N-1} f(x) \quad (13)$$

turns Eq. (12) into the product

$$\mathbf{M}[(A \otimes B)(x)](N) = \mathbf{M}[A(x)](N) \cdot \mathbf{M}[B(x)](N). \quad (14)$$

Before forming the structure function difference in (10, 11) one has to unfold the nuclear corrections of the deuteron structure functions. The lowest Mellin moment of (11) is given by the polarized Bjorken sum rule [27].

3 The Non-singlet Evolution

The evolution operator of scheme-invariant flavor non-singlet evolution, E_{NS} , is obtained as follows.²

The evolution equation for the non-singlet structure functions can be written as

$$\frac{d}{d \ln(Q^2)} \ln [F^{\text{NS}}(Q^2)] = \frac{d}{d \ln(Q^2)} \ln [C^{\text{NS}}(Q^2)] + \frac{d}{d \ln(Q^2)} \ln [q^{\text{NS}}(Q^2)]. \quad (15)$$

Its solution is given by

$$F^{\text{NS}}(Q^2) = E_{\text{NS}}(Q^2, Q_0^2) \cdot F^{\text{NS}}(Q_0^2). \quad (16)$$

The Wilson coefficient is given by

$$C(Q^2) = 1 + \sum_{k=1}^{\infty} a_s^k(Q^2) C_k, \quad C_k = c_k + h_k(L_c, L_b). \quad (17)$$

Here c_k denote the expansion coefficients of the massless Wilson coefficients and h_k of the massive Wilson coefficient, with

$$L_c = \ln \left(\frac{Q^2}{m_c^2} \right), \quad L_b = \ln \left(\frac{Q^2}{m_b^2} \right) \quad (18)$$

and $m_{c,b}$ are the on-shell charm and bottom quark masses.

In the non-singlet case the heavy flavor corrections contribute from $O(a_s^2)$ onward. One has

$$h_1 = 0 \quad (19)$$

$$h_2 = \hat{h}_2(L_c) + \hat{h}_2(L_b) \quad (20)$$

²Here and below we will work in Mellin N space.

$$h_3 = \hat{h}_3(L_c) + \hat{h}_3(L_b) + \hat{\hat{h}}_3(L_c, L_b), \quad (21)$$

where \hat{h}_i denote the single mass and $\hat{\hat{h}}_3$ the double mass contributions.

One may rewrite the differential operator

$$\frac{d}{d \ln(Q^2)} = \frac{da_s(Q^2)}{d \ln(Q^2)} \cdot \frac{d}{da_s(Q^2)} \quad (22)$$

with

$$\frac{da_s}{d \ln(Q^2)} = - \sum_{k=0}^{\infty} \beta_k a_s^{k+2}. \quad (23)$$

The evolution equation for the non-singlet quark density is given by

$$\frac{d}{da_s} \ln [q^{\text{NS}}(Q^2)] = - \frac{1}{2} \frac{\sum_{k=0}^{\infty} a_s^{k+1} P_k}{\sum_{k=0}^{\infty} \beta_k a_s^{k+2}}, \quad (24)$$

where β_k are expansion coefficients of the QCD- β function and P_k are the splitting functions. The anomalous dimensions are related to the splitting functions³ by

$$\gamma_{ij}^{(k)}(N) = - \int_0^1 dx x^{N-1} P_{ij}^{(k)}(x). \quad (25)$$

The solution of Eq. (15) to N³LO reads

$$\begin{aligned} E_{\text{NS}}(Q^2, Q_0^2) &= \left(\frac{a}{a_0}\right)^{-\frac{F_0}{2\beta_0}} \left\{ 1 + \frac{a - a_0}{2\beta_0^2} \left\{ \left[1 + a^2 C_2(Q^2) - a_0^2 C_2(Q_0^2) \right] (2\beta_0^2 C_1 - \beta_0 P_1 + \beta_1 P_0) \right. \right. \\ &\quad - \frac{(a^2 - a_0^2)}{4\beta_0^3} (2\beta_0^2 C_1 - \beta_0 P_1 + \beta_1 P_0) \left[2\beta_0^3 C_1^2 + \beta_0^2 P_2 - \beta_0 \beta_1 P_1 + (\beta_1^2 - \beta_0 \beta_2) P_0 \right] \\ &\quad + \frac{(a^2 + aa_0 + a_0^2)}{3\beta_0^2} \left[2\beta_0^4 C_1^3 - \beta_0^3 P_3 + \beta_0^2 \beta_1 P_2 + (\beta_0^2 \beta_2 - \beta_0 \beta_1^2) P_1 \right. \\ &\quad \left. \left. + (\beta_0^2 \beta_3 - 2\beta_0 \beta_1 \beta_2 + \beta_1^3) P_0 \right] + \frac{a - a_0}{4\beta_0^2} (2\beta_0^2 C_1 - \beta_0 P_1 + \beta_1 P_0)^2 \right. \\ &\quad \left. + \frac{(a - a_0)^2}{24\beta_0^4} (2\beta_0^2 C_1 - \beta_0 P_1 + \beta_1 P_0)^3 - \frac{a + a_0}{2\beta_0} \left[2\beta_0^3 C_1^2 + \beta_0^2 P_2 - \beta_0 \beta_1 P_1 \right. \right. \\ &\quad \left. \left. + P_0 (\beta_1^2 - \beta_0 \beta_2) \right] \right\} + a^2 C_2(Q^2) - a_0^2 C_2(Q_0^2) - C_1 \left[a^3 C_2(Q^2) - a_0^3 C_2(Q_0^2) \right] \\ &\quad \left. + a^3 C_3(Q^2) - a_0^3 C_3(Q_0^2) \right\} \quad (26) \end{aligned}$$

and $a = a_s(Q^2)$, $a_0 = a_s(Q_0^2)$ and $P_i(N) \equiv P_i$ denotes the Mellin transform of $P_i(z)$. The heavy quark contributions to the Wilson coefficients are given by [15, 16, 30, 31]

$$\hat{h}_2^{(Q)} = -\frac{\beta_{0,Q}}{4} P_{qq}^{(0)} \ln^2 \left(\frac{Q^2}{m^2} \right) + \frac{1}{2} \hat{P}_{qq}^{(1),\text{NS}} \ln \left(\frac{Q^2}{m^2} \right) + a_{qq}^{(2),\text{NS}} + \frac{\beta_{0,Q}}{4} \zeta_2 P_{qq}^{(0)} + \hat{C}_q^{(2),\text{NS}} \quad (27)$$

³Our normalizations are such that a factor of two has to be applied to those given in [28, 29].

$$\begin{aligned}
\hat{h}_3^{(Q)} &= -\frac{1}{6}P_{qq}^{(0)}\beta_{0,Q}(\beta_0 + 2\beta_{0,Q})\ln^3\left(\frac{Q^2}{m^2}\right) + \frac{1}{4}\left[-2P_{qq}^{(1),\text{NS}}\beta_{0,Q} + 2\hat{P}_{qq}^{(1),\text{NS}}(\beta_0 + \beta_{0,Q})\right. \\
&\quad \left.-\beta_{1,Q}P_{qq}^{(0)}\right]\ln^2\left(\frac{Q^2}{m^2}\right) - \frac{1}{2}\left[-\hat{P}_{qq}^{(2),\text{NS}} - \left(4a_{qq,Q}^{(2),\text{NS}} + \zeta_2\beta_{0,Q}P_{qq}^{(0)}\right)(\beta_0 + \beta_{0,Q})\right. \\
&\quad \left.-P_{qq}^{(0)}\beta_{1,Q}^{(1)}\right]\ln\left(\frac{Q^2}{m^2}\right) + 4\bar{a}_{qq,Q}^{(2),\text{NS}}(\beta_0 + \beta_{0,Q}) + P_{qq}^{(0)}\beta_{1,Q}^{(2)} + \frac{1}{6}P_{qq}^{(0)}\beta_0\beta_{0,Q}\zeta_3 \\
&\quad + \frac{1}{4}P_{qq}^{(1),\text{NS}}\beta_{0,Q}\zeta_2 - 2\delta m_1^{(1)}\beta_{0,Q}P_{qq}^{(0)} - \delta m_1^{(0)}\hat{P}_{qq}^{(1),\text{NS}} + 2\delta m_1^{(-1)}a_{qq,Q}^{(2),\text{NS}} + a_{qq,Q}^{(3),\text{NS}} \\
&\quad + \left[-\frac{\beta_{0,Q}}{4}P_{qq}^{(0)}\ln^2\left(\frac{Q^2}{m^2}\right) + \frac{1}{2}\hat{P}_{qq}^{(1),\text{NS}}\ln\left(\frac{Q^2}{m^2}\right) + a_{qq}^{(2),\text{NS}} + \frac{\beta_{0,Q}}{4}\zeta_2P_{qq}^{(0)}\right]C_q^{(1),\text{NS}} \\
&\quad + \hat{C}_q^{(3),\text{NS}}. \tag{28}
\end{aligned}$$

The two-mass three-loop contributions [32] read

$$\begin{aligned}
\hat{h}_3^{\text{NS}} &= P_{qq}^{(0)}\beta_{0,Q}^2\left[\frac{2}{3}(L_c^3 + L_b^3) + \frac{1}{2}(L_c^2L_b + L_cL_b^2)\right] - \beta_{0,Q}\hat{P}_{qq}^{(1),\text{NS}}(L_c^2 + L_b^2) - \left[4a_{qq,Q}^{(2),\text{NS}}\beta_{0,Q}\right. \\
&\quad \left.-\frac{1}{2}\beta_{0,Q}^2P_{qq}^{(0)}\zeta_2\right](L_c + L_b) + 8\bar{a}_{qq,Q}^{(2),\text{NS}}\beta_{0,Q} + \tilde{a}_{qq,Q}^{(3),\text{NS}}(m_c, m_b, Q^2). \tag{29}
\end{aligned}$$

The two-mass term is the same in the unpolarized and polarized case. In the r.h.s. of Eqs. (27–29) we define

$$\hat{f}(x, N_F) = f(x, N_F + 1) - f(x, N_F). \tag{30}$$

In the $\overline{\text{MS}}$ scheme the iterative solution for $a_s(Q^2)$ is [33]

$$\begin{aligned}
a_s(Q^2) &= \frac{1}{\beta_0 L} - \frac{\beta_1}{\beta_0^3 L^2} \ln(L) + \frac{1}{\beta_0^3 L^3} \left[\frac{\beta_1^2}{\beta_0^2} (\ln^2(L) - \ln(L) - 1) + \frac{\beta_2}{\beta_0} \right] \\
&\quad + \frac{1}{\beta_0^4 L^4} \left[\frac{\beta_1^3}{\beta_0^3} \left(-\ln^3(L) + \frac{5}{2} \ln^2(L) + 2 \ln(L) - \frac{1}{2} \right) - 3 \frac{\beta_1 \beta_2}{\beta_0^2} \ln(L) + \frac{\beta_3}{2\beta_0} \right], \tag{31}
\end{aligned}$$

with $L = \ln(Q^2/\Lambda_{\text{QCD}}^2)$. Here the integration constant for solving (23) is chosen by $(\beta_1/\beta_0^2)\ln(\beta_0)$ [34]. The expansion coefficients of the β -function to N³LO were calculated in [35]. The flavor matching conditions were given in [33]. The expansion coefficients of the renormalized mass were given in [36, 37]. The constant and $O(\varepsilon)$ parts of the massive unrenormalized operator matrix elements at $O(a_s^k)$ are denoted by $a_{ij}^{(k)}$ and $\bar{a}_{ij}^{(k)}$, respectively, cf. [11, 12, 38, 39].

The three-loop massless Wilson coefficients are expressed by effective representations. Otherwise we use the analytic Mellin space representations. After algebraic reduction [40], they depend on 32 harmonic sums [41, 42] up to weight $w=6$ only, which is particular to the flavor non-singlet case to three-loop orders. Other massive Wilson coefficients have a more involved structure [43–46]. It is useful to represent harmonic sums with an alternating index by their Mellin transform, to eliminate spurious $(-1)^N$ terms [42] before performing the analytic continuation from even or odd integers to the complex plane. The singularities of the problem are located at the non-positive integers, around which the contour integral is performed, cf. [47–50]. For the analytic continuation we follow Refs. [51, 52].

In the case of the structure function F_2 the non-singlet anomalous dimensions are $P^{\text{NS},+}$ and the expansion coefficients of the Wilson coefficient up to c_3 were calculated in [53]. In the case of the structure function g_1 the anomalous dimensions are $P^{\text{NS},-}$, cf. [28], and the Wilson coefficient has been given in [54].⁴ Below we will also use the combination

$$F_2^{\text{h}}(N, Q^2) = [E_{\text{NS}} - E_{\text{NS}}|_{\text{h}=0}] F_2(N, Q_0^2). \quad (32)$$

The four-loop non-singlet anomalous dimensions are not yet completely known as a function of N . However, a series of moments has been calculated in [79–84]. We follow the earlier investigation in Ref. [6] and compare these moments with the Padé-approximation

$$P_{qq}^{3,\pm,\text{NS}}(N) \approx \frac{P_{qq}^{2,\pm,\text{NS}}(N)^2}{P_{qq}^{1,\pm,\text{NS}}(N)}, \quad (33)$$

with the exact moments in [79–84] in Table 1. Furthermore, the leading N_F terms for the even moments have been predicted in [85].

From the 2nd moment, which agrees within 21%, cf. also [6], the accuracy improves to 2.2 % for the known even moments at $N = 16$ and to 2.6% for the odd moments at $N = 15$. For the first moment for $\gamma^{-,\text{NS}}$ the Padé-approximation delivers even the correct result, after using the l’Hospital rule.

N	$\delta\gamma^{+,\text{NS}}$	N	$\delta\gamma^{-,\text{NS}}$
2	0.208822541	1	0.0
4	0.123728742	3	0.147102092
6	0.087155544	5	0.101634935
8	0.064949195	7	0.074593595
10	0.049680399	9	0.056598595
12	0.038394815	11	0.043633919
14	0.029638565	13	0.033767853
16	0.022602035	15	0.025956941

Table 1: The relative error comparing the exact moments of the four-loop anomalous dimensions, $\gamma^{(3),\pm,\text{NS}}$, with the Padé approximation (33).

The leading small x terms for $P_3^{\text{NS},+}$ and $P_2^{\text{NS},-}$ have been given in [86] after correcting some misprints there in Ref. [87], see also [88]. However, yet unknown sub-leading terms, having been studied at the known lower orders, are numerically dominant over the leading small x corrections and several of these sub-leading terms are needed, cf. [49, 87], to be calculated to obtain reliable quantitative prediction in this region of x . Table 1 shows that (33) provides an excellent model. The earlier assumption of an error of 100% in [6] on this relation has been very conservative and still led to an error in Λ_{QCD} of 2 MeV only, which could now be improved in principle. Yet the experimental accuracy at this level cannot be reached at present, since the current experimental error amounts to $\delta\Lambda_{\text{QCD}} = 26$ MeV [6].

⁴Lower orders of the non-singlet anomalous dimensions and the massless non-singlet Wilson coefficients have been calculated in [15, 55–64] and [63, 65–68] and in the polarized case in [69–74] and [75–78].

4 Numerical Results

The measured input distributions contain correlated errors, which are parameterized by the respective fits. cf. [6, 19, 89]. Their evolution, including the corresponding correlation matrix, has to be performed to provide the error prediction of the structure function at every fixed value of $\Lambda_{\text{QCD}}, m_c$ and m_b respectively. Here one may use the corresponding formulae for the correlated error propagation given in Ref. [6] and extensions of them, which are straightforward. Within future data analyses one will probably import the values of the heavy quark masses from the world data analyses. For the charm quark mass it has already been shown that its value obtained from deep-inelastic scattering data fully agrees with other precision measurements [90]. In our illustrations we will use the values $m_c = 1.59$ GeV [90] and $m_b = 4.78$ GeV [91].

For the input distribution in the unpolarized case we refer to the one of Ref. [6]

$$F_2^{\text{NS}}(x, Q_0^2) = C^{\text{NS}}(x, Q_0^2) \otimes xq^{\text{NS}}(x, Q_0^2) \quad (34)$$

$$xq^{\text{NS}}(x, Q_0^2) = \frac{1}{3} \left[0.262 x^{0.298} (1-x)^{4.032} (1 + 6.042\sqrt{x} + 35.49x) \right. \\ \left. - 1.085 x^{0.5} (1-x)^{5.921} (1 - 3.618\sqrt{x} + 16.41x) \right] \quad (35)$$

at $Q_0^2 = 4$ GeV². In the polarized case we use the fit to $xg_1^{\text{NS}}(x, Q_0^2)$ of the structure function of Ref. [89] at $Q_0^2 = 10$ GeV²,

$$xg_1^{\text{NS}}(x, Q_0^2) = 2.4312 \cdot 10^{-5} x^{-0.38573} (1-x)^{2.69522} \\ \times (-1 + 279.624\sqrt{x} + 1239.76x + 7053.93x^{3/2} + 1866.208x^2) \quad (36)$$

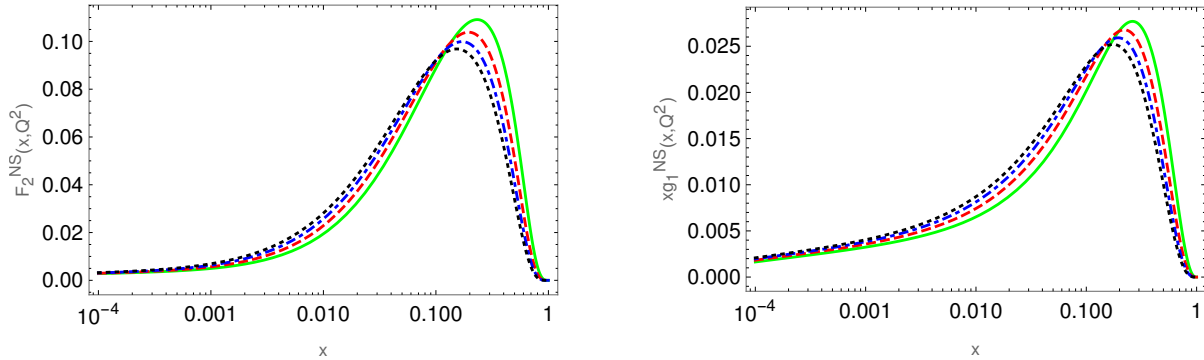


Figure 1: Left: The structure function F_2^{NS} at N³LO. Right: The structure function xg_1^{NS} at N³LO. Full lines: $Q^2 = 10$ GeV²; dashed lines: 100 GeV²; dash-dotted lines: 1000 GeV²; dotted lines: 10000 GeV².

In the numeric illustration our reference starting scale will be chosen to be $Q_0^2 = 10$ GeV² both in the unpolarized and polarized case. In Figures 1 we show the scheme-invariant evolution of the non-singlet structure functions F_2^{NS} and xg_1^{NS} in the kinematic region $Q^2 \in [10, 10^4]$ GeV². In Figures 2 we expand the representation for the region of larger values of x . Both structure functions show a falling behaviour both towards small and large values of x . To improve the measurement of the strong coupling constant future measurements of these structure functions are necessary at the 1% level.

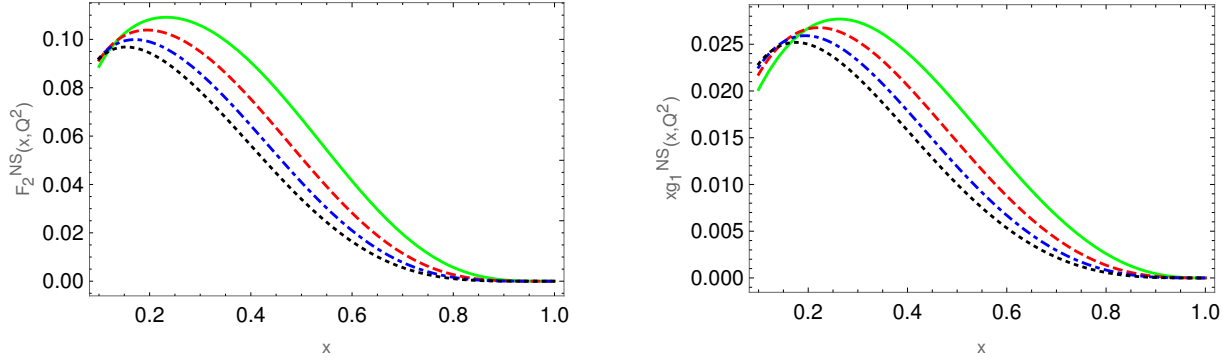


Figure 2: The same as Figure 1 but with expanded large x region.

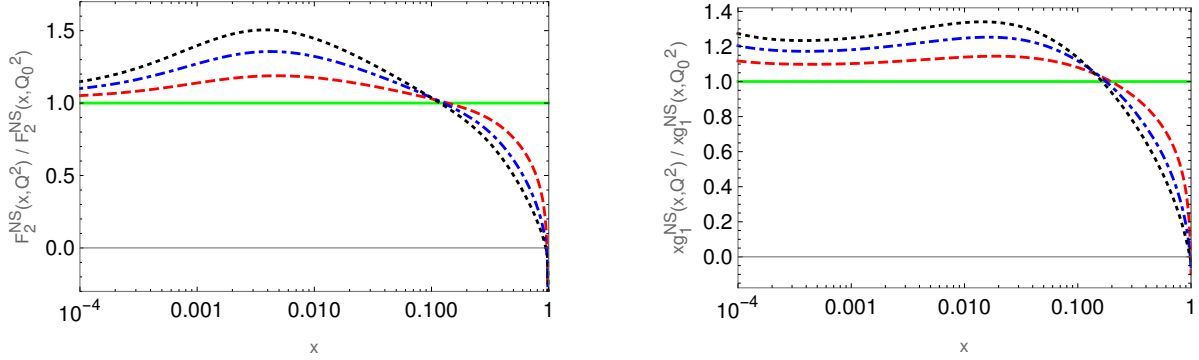


Figure 3: Left: The relative contribution of F_2^{NS} in the evolution from $Q^2 = 10 \text{ GeV}^2$ to 10000 GeV^2 . Right: The same for the structure function xg_1^{NS} .

In Figures 3 we illustrate the relative effect of the scale evolution in Q^2 both for F_2^{NS} and xg_1^{NS} comparing to the starting scale Q_0^2 . There is a fixpoint at $x_0 \sim 0.1$ with a positive evolution with Q^2 at lower x and a negative evolution at larger x .

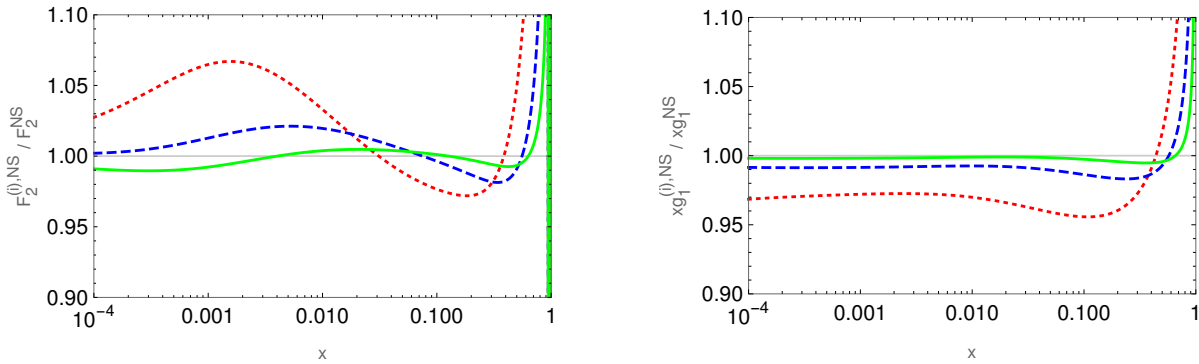


Figure 4: Left: The relative contributions from LO (dotted lines), NLO (dashed lines) and NNLO (full lines) to the structure function F_2^{NS} at $N^3\text{LO}$ at $Q^2 = 100 \text{ GeV}^2$ as an example. Right: The same for the structure function xg_1^{NS} .

In Figures 4 we show the ratio of the results obtained at leading order (LO), next-to-leading order (NLO), and next-to-next-to leading order (NNLO) to the N³LO results at $Q^2 = 100 \text{ GeV}^2$. This illustrates the convergence of the perturbative series of the corrections and the necessity to include N³LO corrections at an accuracy of the data in the 1% region.

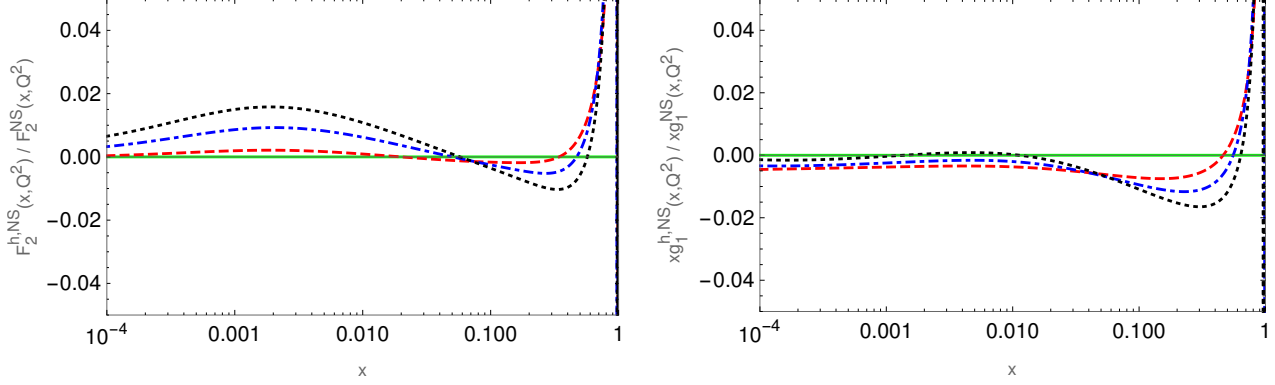


Figure 5: Left: The relative contribution of the heavy flavor contributions due to c and b quarks to the structure function F_2^{NS} at N³LO; dashed lines: 100 GeV^2 ; dashed-dotted lines: 1000 GeV^2 ; dotted lines: 10000 GeV^2 . Right: The same for the structure function xg_1^{NS} at N³LO.

In Figures 5 we illustrate the relative size of the heavy flavor parts for the same region in Q^2 in the unpolarized and polarized cases. In the important region $x \leq 0.4$ the heavy flavor corrections reach the size of $\sim 1\%$. Therefore they are of importance for precision analyses. Larger relative effects are found at larger values of x . There, however, the structure functions and their heavy flavor content drop rapidly.

In Figures 6 we illustrate the effect of the half difference if putting $P_{qq}^{3,\pm,\text{NS}} = 2P_{qq}^{2,\pm,\text{NS}^2} / P_{qq}^{2,\pm,\text{NS}}$ and $P_{qq}^{3,\pm,\text{NS}} = 0$ for both F_2^{NS} and xg_1^{NS} . This rescaled correction is in the sub-percent range. Moreover, the impact on Λ_{QCD} comes from the slope in Q^2 which is seen to be rather small.

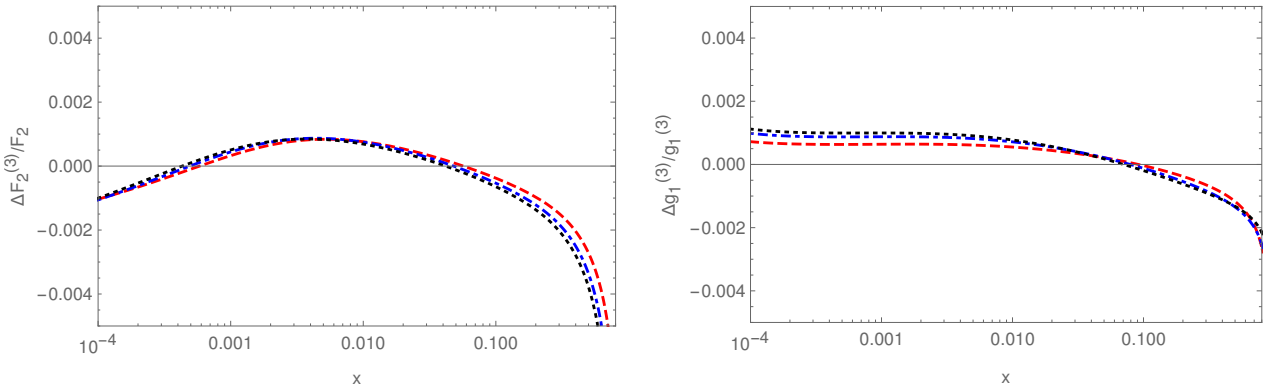


Figure 6: The effect of the variation of $P_{qq}^{3,\pm,\text{NS}}$ around the value in Eq. (33) by $\pm 100\%$. Dashed lines: $Q^2 = 100 \text{ GeV}^2$, Dash-dotted lines: $Q^2 = 1000 \text{ GeV}^2$; Dotted lines: $Q^2 = 10000 \text{ GeV}^2$. Left: F_2^{NS} ; Right: xg_1^{NS} .

5 Conclusions

We have calculated the evolution of flavor non-singlet structure functions in the unpolarized and polarized case, which become available in high luminosity experiments performed both on proton and deuteron data with comparable statistics. The evolution has been performed in Mellin N space using our code `QCDEVO`. Referring to the structure functions directly has the advantage that the input distributions are measured. The evolution does only depend on the QCD scale Λ_{QCD} and the heavy quark masses m_c and m_b , the latter of which have been measured very precisely already [91]. Therefore, this method allows for a one parameter fit of Λ_{QCD} only, and provides a method which is systematically very stable. The input, after corrections for the deuteron wave function, is given by the difference of two structure functions which both can be measured at very high statistics at future facilities [21,22]. The heavy flavor corrections amount to a contribution of $\sim 1\%$ in the region $x < 0.4$.

Let us finally mention that one may also consider the scheme-invariant singlet evolution [62, 65, 92–100] in addition to the one in the flavor non-singlet case, provided the corresponding flavor decomposition can be carried out. This will usually require more than just the deep-inelastic data, because of the sea-quark combinations. A possible way would consist in referring to the Drell–Yan cross section here. Already this part complicates the analysis. Furthermore, one needs to measure the slope $\partial F_i / \partial \ln(Q^2)$ at the input scale Q_0^2 together with $F_i(Q_0^2)$ in an uncorrelated way. A second possibility would consist in using the pair $F_2^{\text{S}}(Q_0^2), F_L^{\text{S}}(Q_0^2)$. However, the measurement of the structure function F_L^{S} is much more difficult than that of F_2^{S} and in the past not enough statistics has been collected in this case, cf. [101–103], see, however, [104]. To perform the necessary flavor decomposition, one needs to perform all these measurements both at proton and deuteron targets. By scheme-invariant evolution the fitting problem of input distributions does not exist and no further optimization by neural network techniques is necessary since the input distribution is fully determined by its measurement.

Acknowledgment. We would like to thank K. Chetyrkin, K. Schönwald, and A. Vogt for discussions. This project has received funding from the European Union’s Horizon 2020 research and innovation programme under the Marie Skłodowska-Curie grant agreement No. 764850, SAGEX.

References

- [1] S. Bethke *et al.*, Workshop on Precision Measurements of α_s , arXiv:1110.0016 [hep-ph].
- [2] S. Moch *et al.*, High precision fundamental constants at the TeV scale, arXiv:1405.4781 [hep-ph].
- [3] S. Alekhin, J. Blümlein and S. O. Moch, Mod. Phys. Lett. A **31** (2016) no.25, 1630023.
- [4] A. Accardi *et al.*, Eur. Phys. J. C **76** (2016) no.8, 471 [arXiv:1603.08906 [hep-ph]]; S. Alekhin, J. Blümlein, S. Moch and R. Placakyte, Phys. Rev. D **96** (2017) no.1, 014011 [arXiv:1701.05838 [hep-ph]].
- [5] P.A. Baikov, K.G. Chetyrkin, J.H. Kühn and J. Rittinger, Phys. Rev. Lett. **108** (2012) 222003 [arXiv:1201.5804 [hep-ph]].
- [6] J. Blümlein, H. Böttcher and A. Guffanti, Nucl. Phys. B **774** (2007) 182–207 [hep-ph/0607200].
- [7] J. Blümlein and H. Böttcher, Proc. DIS 2012, Bonn, 237–241 (DESY, Hamburg, 2012) [arXiv:1207.3170 [hep-ph]].
- [8] F. Eisele, Rept. Prog. Phys. **49** (1986) 233–339.
- [9] A.C. Benvenuti *et al.* [BCDMS Collaboration], Phys. Lett. B **223** (1989) 490–496.
- [10] J. Blümlein, M. Klein, G. Ingelman and R. Rückl, Z. Phys. C **45** (1990) 501–513.

- [11] M. Buza, Y. Matiounine, J. Smith, R. Migneron and W.L. van Neerven, Nucl. Phys. B **472** (1996) 611–658 [hep-ph/9601302].
- [12] I. Bierenbaum, J. Blümlein and S. Klein, Nucl. Phys. B **780** (2007) 40–75 [hep-ph/0703285].
- [13] M. Buza, Y. Matiounine, J. Smith and W.L. van Neerven, Nucl. Phys. B **485** (1997) 420–456 [hep-ph/9608342].
- [14] A. Behring, I. Bierenbaum, J. Blümlein, A. De Freitas, S. Klein and F. Wißbrock, Eur. Phys. J. C **74** (2014) no.9, 3033 [arXiv:1403.6356 [hep-ph]].
- [15] J. Ablinger, A. Behring, J. Blümlein, A. De Freitas, A. Hasselhuhn, A. von Manteuffel, M. Round, C. Schneider, and F. Wißbrock, Nucl. Phys. B **886** (2014) 733–823 [arXiv:1406.4654 [hep-ph]].
- [16] A. Behring, J. Blümlein, A. De Freitas, A. von Manteuffel and C. Schneider, Nucl. Phys. B **897** (2015) 612–644 [arXiv:1504.08217 [hep-ph]].
- [17] J. Blümlein, A. De Freitas, M. Saragnese, C. Schneider and K. Schönwald, *The Logarithmic Contributions to the Polarized $O(\alpha_s^3)$ Asymptotic Massive Wilson Coefficients and Operator Matrix Elements in Deeply Inelastic Scattering*, Phys. Rev. D (2021) in print [arXiv:2105.09572 [hep-ph]].
- [18] S.I. Alekhin and J. Blümlein, Phys. Lett. B **594** (2004) 299–307 [hep-ph/0404034].
- [19] S. Alekhin, J. Blümlein and S. Moch, Phys. Rev. D **86** (2012) 054009 [arXiv:1202.2281 [hep-ph]].
- [20] J. Blümlein and H. Böttcher, Phys. Lett. B **662** (2008) 336–340 [arXiv:0802.0408 [hep-ph]].
- [21] D. Boer *et al.*, Gluons and the quark sea at high energies: Distributions, polarization, tomography, arXiv:1108.1713 [nucl-th].
- [22] J.L. Abelleira Fernandez *et al.* [LHeC Study Group], J. Phys. G **39** (2012) 075001 [arXiv:1206.2913 [physics.acc-ph]].
- [23] A. Vogt, Comput. Phys. Commun. **170** (2005) 65–92 [hep-ph/0408244].
- [24] M. Boscolo, J.P. Delahaye and M. Palmer, *The future prospects of muon colliders and neutrino factories*, [arXiv:1808.01858 [physics.acc-ph]].
- [25] J. Blümlein, Prog. Part. Nucl. Phys. **69** (2013) 28–84 [arXiv:1208.6087 [hep-ph]].
- [26] N. Schmitz, *Neutrino Physik*, (Teunber, Stuttgart, 1997).
- [27] J. D. Bjorken, Phys. Rev. D **1** (1970) 1376–1379.
- [28] S. Moch, J.A.M. Vermaseren and A. Vogt, Nucl. Phys. B **688** (2004) 101–134 [hep-ph/0403192].
- [29] A. Vogt, S. Moch and J.A.M. Vermaseren, Nucl. Phys. B **691** (2004) 129–181 [hep-ph/0404111].
- [30] J. Blümlein, G. Falcioni and A. De Freitas, Nucl. Phys. B **910** (2016) 568–617 [arXiv:1605.05541 [hep-ph]].
- [31] I. Bierenbaum, J. Blümlein and S. Klein, Nucl. Phys. B **820** (2009) 417–482 [arXiv:0904.3563 [hep-ph]].
- [32] J. Ablinger, J. Blümlein, A. De Freitas, A. Hasselhuhn, C. Schneider and F. Wißbrock, Nucl. Phys. B **921** (2017) 585–688 [arXiv:1705.07030 [hep-ph]].
- [33] K.G. Chetyrkin, B.A. Kniehl and M. Steinhauser, Phys. Rev. Lett. **79** (1997) 2184–2187 [hep-ph/9706430].
- [34] W.A. Bardeen, A.J. Buras, D.W. Duke and T. Muta, Phys. Rev. D **18** (1978) 3998–4017.
- [35] D.J. Gross and F. Wilczek, Phys. Rev. Lett. **30** (1973) 1343–1346;
H.D. Politzer, Phys. Rev. Lett. **30** (1973) 1346–1349;
W.E. Caswell, Phys. Rev. Lett. **33** (1974) 244–246;
D.R.T. Jones, Nucl. Phys. B **75** (1974) 531–538;
O.V. Tarasov, A.A. Vladimirov and A.Y. Zharkov, Phys. Lett. B **93** (1980) 429–432;
S.A. Larin and J.A.M. Vermaseren, Phys. Lett. B **303** (1993) 334–336 [hep-ph/9302208];
T. van Ritbergen, J.A.M. Vermaseren and S.A. Larin, Phys. Lett. B **400** (1997) 379–384 [hep-ph/9701390];
M. Czakon, Nucl. Phys. B **710** (2005) 485–498 [hep-ph/0411261];
P.A. Baikov, K.G. Chetyrkin and J.H. Kühn, Phys. Rev. Lett. **118** (2017) no.8, 082002 [arXiv:1606.08659 [hep-ph]];
F. Herzog, B. Ruijl, T. Ueda, J.A.M. Vermaseren and A. Vogt, JHEP **02** (2017) 090 [arXiv:1701.01404 [hep-ph]].

- T. Luthe, A. Maier, P. Marquard and Y. Schröder, *JHEP* **10** (2017) 166 [arXiv:1709.07718 [hep-ph]]; K.G. Chetyrkin, G. Falcioni, F. Herzog and J.A.M. Vermaseren, *JHEP* **10** (2017) 179 [arXiv:1709.08541 [hep-ph]].
- [36] D.J. Broadhurst, N. Gray and K. Schilcher, *Z. Phys. C* **52** (1991) 111–122.
- [37] N. Gray, D.J. Broadhurst, W. Grafe and K. Schilcher, *Z. Phys. C* **48** (1990) 673–680.
- [38] I. Bierenbaum, J. Blümlein, S. Klein and C. Schneider, *Nucl. Phys. B* **803** (2008) 1–41 [arXiv:0803.0273 [hep-ph]].
- [39] I. Bierenbaum, J. Blümlein, A. De Freitas, S. Klein, and K. Schönwald, *The $O(\alpha_s^2)$ Polarized Heavy Flavor Corrections to Deep-Inelastic Scattering at $Q^2 \gg m^2$* , DESY 15–004.
- [40] J. Blümlein, *Comput. Phys. Commun.* **159** (2004) 19–54 [hep-ph/0311046].
- [41] J.A.M. Vermaseren, *Int. J. Mod. Phys. A* **14** (1999) 2037–2076 [hep-ph/9806280].
- [42] J. Blümlein and S. Kurth, *Phys. Rev. D* **60** (1999) 014018 [hep-ph/9810241].
- [43] J. Ablinger, A. Behring, J. Blümlein, A. De Freitas, A. von Manteuffel and C. Schneider, *Nucl. Phys. B* **890** (2014) 48–151 [arXiv:1409.1135 [hep-ph]].
- [44] J. Ablinger, J. Blümlein, A. De Freitas, A. Hasselhuhn, A. von Manteuffel, M. Round and C. Schneider, *Nucl. Phys. B* **885** (2014) 280–317 [arXiv:1405.4259 [hep-ph]].
- [45] J. Blümlein, J. Ablinger, A. Behring, A. De Freitas, A. von Manteuffel, C. Schneider and C. Schneider, *PoS (QCDEV2017) 031* [arXiv:1711.07957 [hep-ph]].
- [46] J. Ablinger et al., DESY 15–112.
- [47] M. Diemoz, F. Ferroni, E. Longo and G. Martinelli, *Z. Phys. C* **39** (1988) 21–37.
- [48] M. Glück, E. Reya and A. Vogt, *Z. Phys. C* **48** (1990) 471–482.
- [49] J. Blümlein and A. Vogt, *Phys. Rev. D* **58** (1998) 014020 [hep-ph/9712546].
- [50] R.K. Ellis, Z. Kunszt and E.M. Levin, *Nucl. Phys. B* **420** (1994) 517–549, Erratum: [*Nucl. Phys. B* **433** (1995) 498].
- [51] J. Blümlein, *Comput. Phys. Commun.* **180** (2009) 2218–2249 [arXiv:0901.3106 [hep-ph]].
- [52] J. Blümlein, *Clay Math. Proc.* **12** (2010) 167–188 [arXiv:0901.0837 [math-ph]].
- [53] J.A.M. Vermaseren, A. Vogt and S. Moch, *Nucl. Phys. B* **724** (2005) 3–182 [hep-ph/0504242].
- [54] S. Moch, J.A.M. Vermaseren and A. Vogt, *Nucl. Phys. B* **813** (2009) 220–258 [arXiv:0812.4168 [hep-ph]].
- [55] D.J. Gross and F. Wilczek, *Phys. Rev. D* **8** (1973) 3633–3652.
- [56] H. Georgi and H.D. Politzer, *Phys. Rev. D* **9** (1974) 416–420.
- [57] E.G. Floratos, D.A. Ross and C.T. Sachrajda, *Nucl. Phys. B* **129** (1977) 66–88 [Erratum-ibid. *B* **139** (1978) 545–546].
- [58] A. Gonzalez-Arroyo, C. Lopez and F.J. Yndurain, *Nucl. Phys. B* **153** (1979) 161–186.
- [59] A. Gonzalez-Arroyo, C. Lopez and F.J. Yndurain, *Nucl. Phys. B* **159** (1979) 512–527.
- [60] G. Curci, W. Furmanski and R. Petronzio, *Nucl. Phys. B* **175** (1980) 27–92.
- [61] E.G. Floratos, R. Lacaze and C. Kounnas, *Phys. Lett.* **98B** (1981) 89–95.
- [62] E.G. Floratos, C. Kounnas and R. Lacaze, *Nucl. Phys. B* **192** (1981) 417–462.
- [63] S. Moch and J.A.M. Vermaseren, *Nucl. Phys. B* **573** (2000) 853–907 [hep-ph/9912355].
- [64] A. Behring, J. Blümlein, A. De Freitas, A. Goedicke, S. Klein, A. von Manteuffel, C. Schneider and K. Schönwald, *Nucl. Phys. B* **948** (2019) 114753 [arXiv:1908.03779 [hep-ph]].
- [65] W. Furmanski and R. Petronzio, *Z. Phys. C* **11** (1982) 293–314.
- [66] W.L. van Neerven and E.B. Zijlstra, *Phys. Lett. B* **272** (1991) 127–133.
- [67] E. B. Zijlstra and W. L. van Neerven, *Phys. Lett. B* **297** (1992) 377–384.

- [68] E. B. Zijlstra and W. L. van Neerven, Nucl. Phys. B **383** (1992) 525–574.
- [69] K. Sasaki, Prog. Theor. Phys. **54** (1975) 1816–1827.
- [70] M.A. Ahmed and G.G. Ross, Phys. Lett. **56B** (1975) 385–390.
- [71] G. Altarelli and G. Parisi, Nucl. Phys. B **126** (1977) 298–318.
- [72] R. Mertig and W. L. van Neerven, Z. Phys. C **70** (1996) 637–654 [hep-ph/9506451].
- [73] W. Vogelsang, Phys. Rev. D **54** (1996) 2023–2029 [hep-ph/9512218].
- [74] W. Vogelsang, Nucl. Phys. B **475** (1996) 47–72 [hep-ph/9603366].
- [75] E.B. Zijlstra and W.L. van Neerven, Nucl. Phys. B **417** (1994) 61–100 Errata: [Nucl. Phys. B **426** (1994) 245]; [Nucl. Phys. B **773** (2007) 105-106]; [Nucl. Phys. B **501** (1997) 599].
- [76] J. Kodaira, S. Matsuda, T. Muta, K. Sasaki and T. Uematsu, Phys. Rev. D **20** (1979) 627–629.
- [77] J. Kodaira, S. Matsuda, K. Sasaki and T. Uematsu, Nucl. Phys. B **159** (1979) 99–124.
- [78] I. Antoniadis and C. Kounnas, Phys. Rev. D **24** (1981) 505–525.
- [79] P.A. Baikov and K.G. Chetyrkin, Nucl. Phys. Proc. Suppl. **160** (2006) 76–79.
- [80] P.A. Baikov, K.G. Chetyrkin and J.H. Kühn, Nucl. Part. Phys. Proc. **261-262** (2015) 3–18 [arXiv:1501.06739 [hep-ph]].
- [81] V.N. Velizhanin, *Four loop anomalous dimension of the third and fourth moments of the non-singlet twist-2 operator in QCD*, arXiv:1411.1331 [hep-ph].
- [82] B. Ruijl, T. Ueda, J.A.M. Vermaseren, J. Davies and A. Vogt, PoS (LL2016) 071 [arXiv:1605.08408 [hep-ph]].
- [83] J. Davies, A. Vogt, B. Ruijl, T. Ueda and J.A.M. Vermaseren, Nucl. Phys. B **915** (2017) 335–362 [arXiv:1610.07477 [hep-ph]].
- [84] S. Moch, B. Ruijl, T. Ueda, J.A.M. Vermaseren and A. Vogt, JHEP **1710** (2017) 041 [arXiv:1707.08315 [hep-ph]].
- [85] J.A. Gracey, Phys. Lett. B **322** (1994) 141–146 [hep-ph/9401214].
- [86] R. Kirschner and L.N. Lipatov, Nucl. Phys. B **213** (1983) 122–148.
- [87] J. Blümlein and A. Vogt, Phys. Lett. B **370** (1996) 149–155 [hep-ph/9510410].
- [88] J. Bartels, B.I. Ermolaev and M.G. Ryskin, Z. Phys. C **70** (1996) 273–280 [hep-ph/9507271].
- [89] J. Blümlein and H. Böttcher, Nucl. Phys. B **841** (2010) 205–230 [arXiv:1005.3113 [hep-ph]].
- [90] S. Alekhin, J. Blümlein, K. Daum, K. Lipka and S. Moch, Phys. Lett. B **720** (2013) 172–176 [arXiv:1212.2355 [hep-ph]].
- [91] P.A. Zyla et al. (Particle Data Group), Prog. Theor. Exp. Phys. 2020, 083C01 (2020) and 2021 update.
- [92] W.A. Bardeen and A.J. Buras, Phys. Lett. B **86** (1979) 61–66, Erratum: [Phys. Lett. B **90** (1980) 485].
- [93] A.J. Buras, Rev. Mod. Phys. **52** (1980) 199–276.
- [94] M. Glück and E. Reya, Phys. Rev. D **25** (1982) 1211–1217.
- [95] G. Grunberg, Phys. Rev. D **29** (1984) 2315–2338.
- [96] S. Catani, Z. Phys. C **75** (1997) 665–678 [hep-ph/9609263].
- [97] R.S. Thorne, Nucl. Phys. B **512** (1998) 323–392 [hep-ph/9710541].
- [98] J. Blümlein, V. Ravindran and W.L. van Neerven, Nucl. Phys. B **586** (2000) 349–381 [hep-ph/0004172].
- [99] F.J. Yndurain *The Theory of Quark and Gluon Interactions*, (Springer, Berlin, 1999), 3rd Edition.
- [100] J. Blümlein and A. Guffanti, Nucl. Phys. Proc. Suppl. **152** (2006) 87–91 [hep-ph/0411110].
- [101] C. Adloff *et al.* [H1], Phys. Lett. B **393** (1997), 452-464 [arXiv:hep-ex/9611017 [hep-ex]].
- [102] V. Andreev *et al.* [H1], Eur. Phys. J. C **74** (2014) no.4, 2814 [arXiv:1312.4821 [hep-ex]].
- [103] S. Chekanov *et al.* [ZEUS], Phys. Lett. B **682** (2009), 8-22 [arXiv:0904.1092 [hep-ex]].
- [104] P. Agostini *et al.* [LHeC and FCC-he Study Group], *The Large Hadron-Electron Collider at the HL-LHC*, arXiv:2007.14491 [hep-ex].